Eur. Phys. J. D (2023)77:93
https://doi.org/10.1140/epjd/s10053-023-00671-z

THE EUROPEAN PHYSICAL JOURNAL D

Regular Article – Atomic Physics

On the sensitivity of uranium opacity with respect to the atomic properties in the context of kilonova emission modeling

Jérôme Deprince[1,2,a], Helena Carvajal Gallego[2,b], Michel Godefroid[3,c], Stéphane Goriely[1,d], Patrick Palmeri[2,e], and Pascal Quinet[2,4,f]

[1] Institut d'Astronomie et d'Astrophysique, Université Libre de Bruxelles, 1050 Brussels, Belgium
[2] Physique Atomique et Astrophysique, Université de Mons, 7000 Mons, Belgium
[3] SQUARES, Université Libre de Bruxelles, 1050 Brussels, Belgium
[4] IPNAS, Université de Liège, Sart Tilman, 4000 Liège, Belgium

Received 24 March 2023 / Accepted 10 May 2023

Abstract. In this study, the sensitivity of the opacities with respect to the atomic parameters is investigated in the case of weakly charged uranium ions. In order to do this, atomic data for U II and U III were calculated with the pseudo-relativistic Hartree–Fock method (HFR) and then, used to determine the expansion opacities for conditions characterizing the ejecta of kilonovae that follow neutron star mergers. In particular, we studied the sensitivity of the opacity with respect to the use of atomic data obtained considering several effects as the ionic core polarization and an adjustment procedure.

1 Introduction

The production of elements heavier than iron in the Universe still remains an unsolved mystery. Half of them are thought to be notably produced by the astrophysical r-process (rapid neutron capture process) [1–3], for which one of the most promising production sites are neutron star mergers (NSMs) [4,5]. In August 2017, gravitational waves generated by a NSM were detected by the LIGO detectors (event GW170817 [6,7]). Its electromagnetic counterpart, the kilonova AT2017gfo, was also observed on this occasion, suggesting the presence of heavy elements in the ejecta [8,9].

Only a single trans-iron element has been definitely identified so far, namely strontium [10,11], while tentative identifications of some lanthanides (La III and Ce III) have been highlighted recently [12]. However, lanthanides and actinides are thought to be produced by r-process during such event [8,13–15]. Kilonova light curve modeling strongly depends on the opacity, which is dominated by lanthanide and actinide opacities, since these elements give rise to millions of radiative transitions because of their complex electronic structures characterized by unfilled nf subshells [15].

Several studies have focused on atomic data computations for opacity determination in weakly and moderately charged lanthanides [16–26]. However, only a few and very recent studies concerned actinide opacities for kilonova modeling purpose [25–27].

In this paper, we focus on atomic data and opacity determination for singly- and doubly ionized uranium (U II and U III), since they are the dominant uranium species predicted to be present in the kilonova ejecta for typical conditions as observed in AT2017gfo 1 day after the merger (i.e., a temperature $T = 5000$ K and a density $\rho = 10^{-13}$ g/cm^3) [20,26]. In order to do this, we used the pseudo-relativistic Hartree–Fock (HFR) method as implemented in Cowan's code [28]. The main purpose of this study is to assess the necessity of taking some extra physical effects into account in our HFR computations, which were not considered in our previous work [26], such as the core polarization effects [29], as well as to evaluate the added value of performing a calibration of our HFR results with respect to experimental data or data available in the literature (which exist only for a very limited number of energy levels).

Helena Carvajal Gallego, Michel Godefroid, St'ephane Goriely, Patrick Palmeri, and Pascal Quinet these authors contributed equally to this work.

[a] e-mail: jerome.deprince@ulb.be (corresponding author)
[b] e-mail: helena.carvajalgallego@umons.ac.be
[c] e-mail: michel.godefroid@ulb.be
[d] e-mail: stephane.goriely@ulb.be
[e] e-mail: patrick.palmeri@umons.ac.be
[f] e-mail: pascal.quinet@umons.ac.be

Published online: 05 June 2023

Table 1 Configurations included in the HFR calculations for U II and U III

U II	$5f^37s^2$, $5f^5$, $5f^46d$, $5f^46f$, $5f^46g$, $5f^47s$, $5f^47p$, $5f^47d$, $5f^47f$, $5f^47g$, $5f^48s$, $5f^48p$, $5f^48d$, $5f^48f$, $5f^48g$,$5f^49s$, $5f^49p$, $5f^49d$, $5f^49f$, $5f^49g$, $5f^36d^2$, $5f^36d7s$, $5f^36d7p$, $5f^36d7d$, $5f^37s7p$, $5f^37s7d$
U III	$5f^4$, $5f^36d$, $5f^36f$, $5f^36g$,$5f^37s$, $5f^37p$, $5f^37d$, $5f^37f$, $5f^37g$, $5f^38s$, $5f^38p$, $5f^38d$, $5f^38f$, $5f^38g$,$5f^39s$, $5f^39p$, $5f^39d$, $5f^39f$, $5f^39g$, $5f^26d^2$, $5f^26d7s$, $5f^26d7p$, $5f^26d7d$,$5f^27s^2$, $5f^27s7p$, $5f^27s7d$

2 Atomic data computations: HFR method

In this work, the HFR approach as developed by Cowan [28] is used to model the atomic structure and compute the radiative parameters in U II and U III. This method is particularly well adapted to obtain large amounts of atomic data as required to compute the opacities. It is based on the minimization of the average energy of each configuration, for which a specific set of orbitals is obtained. Several relativistic corrections (spin-orbit, mass-velocity and Darwin terms) are also considered in a perturbative way.

In the LSJπ representation within the Slater–Condon theory, the atomic wavefunctions (eigenfunctions of the Hamiltonian) Ψ are built as a superposition of N basis wavefunctions φ with the same total angular momentum J and corresponding projection M_J and same parity π, i.e.,

$$\Psi(\gamma J M_J \pi) = \sum_i^N c_i \, \varphi(\gamma_i L_i S_i J M_J \pi), \tag{1}$$

where L_i and S_i are, respectively, the total orbital and the total spin angular momentum quantum numbers of the basis state φ_i and where γ_i stands for the complete relevant information to define each basis wavefunction. Each element of the multiconfiguration Hamiltonian matrix is computed as a sum of products of Racah angular coefficients, v_{ij}^l, and radial Slater and spin-orbit integrals, x_l:

$$\langle i|H|j\rangle = \sum_l v_{ij}^l x_l. \tag{2}$$

As recommended by Cowan [28], scaling factors of 0.85 are applied to the Slater integrals in the present computations. As recently demonstrated, the choice of scaling factors between 0.8 and 0.95 virtually does not affect the computed opacities [24]. The Hamiltonian eigenvalues and eigenstates obtained are then used to compute the radiative parameters such as wavelengths and oscillator strengths for all transitions.

The multiconfiguration models considered for U II and U III are based on one of our recent works [26], where the importance of the multiconfiguration model choice is notably highlighted. The configurations included in the models, which are listed in Table 1, were built by considering single electron excitations from the ground configuration to $n = 6, 7, 8, 9$ shells as well as several double electron excitations toward selected $n = 6$ and $n = 7$ subshells. The main purpose of the present work is to assess the impact of the consideration of several levels of complexity in the atomic data computation, which were not considered in the HFR calculations from [26]. In the latter, the U II and U III atomic data predicted by HFR using the same models as in the present work were of relative poor quality when compared to the few experimental data available in the literature (Selected Constants Energy Levels and Atomic Spectra of Actinides [30], abbreviated as SCASA and available in an online database [31]). The average relative differences between the HFR energy levels obtained in [26] (with the same models as the ones considered in this work) and the values from SCASA were found to be of 31.34% and 25.10% for U II and U III, respectively. In particular, for both ions, the ground levels predicted by HFR did not match the observed ones given in SCASA. In the present study, we investigate if a calibration procedure, on the one hand, and the consideration of an effect not considered in [26], namely the core polarization as described in [29], on the other hand, can significantly affect the resulting opacities for U II and U III. The calibration procedure and the inclusion of core-polarization effects for U II and U III are, respectively, detailed in Sects. 3.2 and 3.3. The sensitivity of the resulting opacities with respect to both of these considerations is evaluated in the corresponding sections.

3 U II and U III opacities

3.1 Expansion formalism

The bound-bound opacities of U II and U III were calculated within the expansion formalism [32–34], as (notably) in [26]. In the latter, the absorption coefficient is given by

$$\kappa^{bb}(\lambda) = \frac{1}{\rho c t} \sum_l \frac{\lambda_l}{\Delta\lambda}(1 - \mathrm{e}^{-\tau_l}), \tag{3}$$

where ρ (in g cm^{-3}) is the ejecta density, c (in cm/s) is the speed of light, t (in s) is the elapsed time since ejection, λ (in Å) is the central wavelength within the region of width $\Delta\lambda$, λ_l are the wavelengths of the lines in this range and τ_l are the corresponding Sobolev opti-

cal depths [35], expressed as

$$\tau_l = \frac{\pi e^2}{m_e c} f_l n_l t \lambda_l, \tag{4}$$

where e (in C) is the elementary charge, m_e (in g) is the electron mass, f_l (dimensionless) is the oscillator strength, and n_l (in cm^{-3}) is the density of the transition lower level. In the local thermodynamic equilibrium (LTE) approximation, n_l can be expressed by means of the Boltzmann distribution according to [36] as

$$n_l = \frac{n}{U(T)} g_l \; e^{-E_l/k_B T}, \tag{5}$$

in which n is the ion density, $U(T)$ is the ion partition function, g_l is the statistical weight of the lower level of the transition, k_B is the Boltzmann constant and T is the temperature.

3.2 Opacity sensitivity to a calibration procedure

Since a non-negligible scattering is observed between the HFR data obtained in our calculations and data from SCASA for both U II and U III (see Sect. 2 and [26]), we tested a calibration of our data by fitting the computed configuration average energies to the ones deduced from SCASA. In this process, a shift is thus applied to the average energies of all configurations to match the ones determined from SCASA before diagonalization of the Hamiltonian. Both eigenvalues (energy levels) and eigenstates are thus affected by such an adjustment (without affecting the orbital basis). For configurations for which no data are available, the same shifts are applied to the average energies of similar configurations (e.g., configurations belonging to the same Rydberg series). As a reminder, the predicted ground states did not match observations from SCASA in both U II and U III (see Sect. 2 and [26]); this configuration average energy adjustment procedure is thus notably carried out in order to solve such energy level inversions.

Figures 1 and 2 show a comparison between the opacity computed with and without considering such a configuration average energy adjustment for U II and U III, respectively, in order to evaluate the sensitivity of the opacity with respect to this calibration procedure and assess if the latter is necessary to properly compute HFR opacities for these ions. The figures clearly show that the above-described calibration procedure used to correct the HFR data has only a very minor impact on the expansion opacities. Even if the energy levels are corrected (as a consequence of the configuration average energy adjustment) and in particular the computed ground level matches the one predicted in SCASA for both U II and U III after calibration, the latter does not significantly affect the expansion opacities determined from the corresponding atomic data. In both cases, the only noticeable difference can be

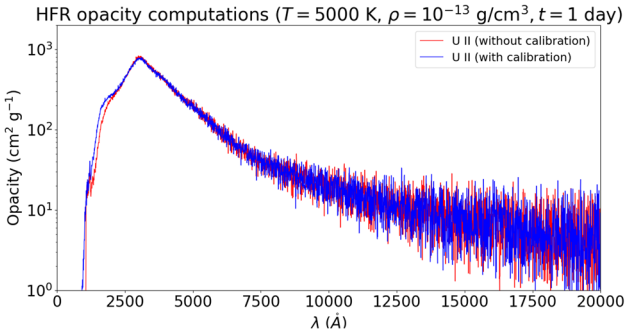

Fig. 1 Effects of the calibration procedure on the opacity computed for U II. Comparison between the opacity obtained without (red curve) and with (blue curve) the adjustment of the configuration average energies of U II

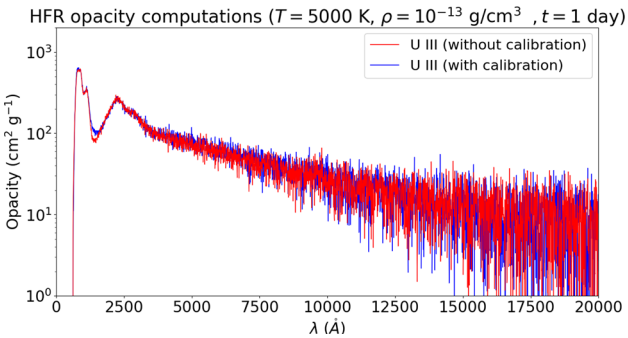

Fig. 2 Same as Fig. 1 for U III

observed at high energies, in the ultraviolet, more precisely for transition wavelengths around 2000 Å. However, since AT2017gfo kilonova spectra were recorded in the spectral region between ultraviolet (3200 Å) and near-infrared (24800 Å) [10], the spectral region corresponding to wavelengths below 3200 Å is not of prime importance for the time being. As a consequence, such a calibration procedure in which the HFR configuration averages energies are shifted to match observed data may not be needed.

3.3 Opacity sensitivity to core-polarization effects

While the largest part of intravalence correlations is represented within a configuration interaction scheme in HFR, a correction can be considered to take core-valence correlations into account. The latter can be approximately represented by a core polarization (CPOL) model potential, first introduced in HFR and described in details in [29]. It was shown that considering CPOL effects in HFR calculations can reduce the predicted oscillator strengths in some cases (e.g., [37,38]). The CPOL potential essentially depends on two parameters: the dipole polarizability of the ionic core, α_d, and its cutoff radius, r_c, often estimated as the outermost core orbital mean radius. In our HFR calculations for U II and U III, the core polarizability values were taken as $\alpha_d = 12.55\ a_0$ and $\alpha_d = 9.79\ a_0$, respectively, according to the values reported in [39]. The cutoff radius of

the ionic core was estimated as the average value of the outermost core orbitals, which leads to $r_c = 1.803\ a_0$ and $r_c = 1.832\ a_0$ for U II and U III, respectively.

It is worth emphasizing that both the ionic cores chosen in the present cases involve the 5f subshell that is partially filled in order to match our multiconfiguration models. More precisely, U IV and U V ionic cores were, respectively, considered for U II and U III ions, corresponding to configurations with partially filled 5f orbitals ($5f^3$ and $5f^2$). As a consequence, valence correlations involving the excitations of electrons occupying the valence orbitals 5f, 6 s and 6p are implicitly included in the CPOL effects. A downside of this CPOL modeling is that the computed dipoles involving the 5f orbital will suffer from overestimated core penetration effects since the 5f orbital average radius is lower than those of the 6 s and 6p orbitals. A way to overcome this problem is the application of a scaling factor to the uncorrected dipole integrals [40]. In our calculations, we thus replace them by the values obtained when scaling down the dipoles computed without CPOL corrections by the mean lowering obtained for the other dipoles. This procedure has already been used with success in multiple cases for weakly charged lanthanides and actinides [37,40–44], providing a good agreement with observations. Moreover, Biémont et al. [37] showed that the choice of the scaling factor applied to dipoles involving the 4f subshell (in Ce III) only weakly affects the computed radiative lifetimes (less than 0.1% when reducing the scaling factor from 0.85 to 0.80). In addition, these computations were in very good agreement with measured radiative lifetimes. Besides, since the cutoff radius is not an unambiguously defined parameter, Gamrath et al. [45] determined that another definition of the core radius corresponding to a value 33% smaller only affects the computed radiative lifetimes by a few percents in the case of neutral lanthanum (La I). As previously observed in other weakly charged ions (e.g., [37,38]), CPOL effects reduce the f-values for both U II and U III by up to 10-15% in both cases. The direct consequence on the opacities can be observed when looking at Figs. 3 and 4, showing the difference between the opacity computed with and without the CPOL correction for U II and U III, respectively, for the conditions expected in the kilonova ejecta 1 day post-merger (a temperature of 5000 K and a density of 10^{-13} g/cm^3). The lowering of the gf-values due to CPOL effects involves a weak lowering of the corresponding opacity in both cases, since U II and U III opacities are both estimated to be reduced by a few percents in average. The impact of the CPOL correction on the opacity for these ions is thus relatively small. Moreover, in light of the approximation used to estimate CPOL correction in the complex case of species with unfilled nf shells (which are actinides, as well as lanthanides) in which the ionic core definition is somewhat nonstandard, in addition to the crude approximations used so far to estimate the opacity in kilonova light curve modeling (e.g., [15]) and to the uncertainties associated with such astrophysical simulations (see, e.g., [14,46,47]), we can conclude that, at least in a first step to model opacities

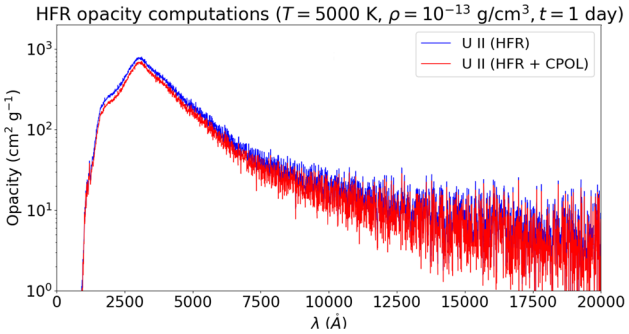

Fig. 3 CPOL effects on the computed opacity for U II, for expected physical conditions of the kilonova ejecta corresponding to 1 day after the merger. The blue curve and the red curve, respectively, represent the U II opacity computed with the atomic data obtained without and with a core-polarization correction

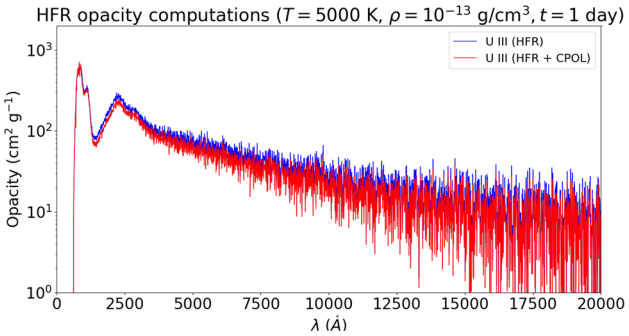

Fig. 4 Same as Fig. 3 for U III

for complex elements such as actinides in the context of kilonova modeling, the consideration of CPOL effects in HFR calculations is not sorely needed. Nevertheless, in a second step, such CPOL correction could be considered for the species that contribute the most to the kilonova opacity.

4 Conclusion

In this work, we investigate the effect of a calibration procedure (in which the configurations average energies are adjusted to match available experimental data) and of the core polarization introduction in the HFR computations on the U II and U III expansion opacities required to model kilonova spectra and light curves. Firstly, we showed that, even if the configuration average energies are adjusted to correct the energy levels and to better match values available in the literature, the resulting computed opacities are virtually not affected by such calibration procedure. As far as the core polarization is concerned, it turned out that the opacity is lowered by a few percents in average in both cases as a result of the oscillator strength lowering due to CPOL effects. Even if the impact is more significant than the one arising from the calibration process,

it is still relatively weak. In addition, in light of the difficulties to introduce such effects in an HFR computations for complex systems as actinides (whose 5f shell is unfilled) as well as of the uncertainties inherent to kilonova modeling, core-polarization effects can be neglected in such complex systems and in this context (at least in a first step), whereas they still could be included in a second step for the elements contributing the most to the kilonova opacity.

Acknowledgements The present work is supported by the FWO and F.R.S.-FNRS under the Excellence of Science (EOS) programme (numbers O.0004.22 and O022818F). HCG is a holder of a FRIA fellowship. SG and PP are Research Associate of the Belgian Fund for Scientific Research F.R.S.-FNRS. PQ is F.R.S.-FNRS Research Director. Computational resources have been provided by the Consortium des Equipements de Calcul Intensif (CECI), funded by the F.R.S. -FNRS under Grant No. 2.5020.11 and by the Walloon Region of Belgium.

Author contributions

All authors contributed equally to the paper.

Data Availability Statement This manuscript has associated data in a data repository. [Authors' comment: Data will be made available upon reasonable request.]

References

1. M. Arnould, S. Goriely, K. Takahashi, Phys. Repts. **450**, 97 (2007)
2. M. Arnould, S. Goriely, Prog. Part. Nucl. Phys. **112**, 103766 (2020)
3. J.J. Cowan, C. Sneden, J.E. Lawler, A. Aprahamian, M. Wiescher, K. Langanke, G. Martínez-Pinedo, F.-K. Thielemann, Rev. Mod. Phys. **93**, 015002 (2021)
4. D. Eichler, M. Livio, T. Piran, D.N. Schramm, Nature **340**, 126 (1989)
5. B.D. Metzger, G. Martinez-Pinedo, S. Darbha et al., MNRAS **406**, 2650 (2010)
6. B.P. Abbott, R. Abbott, T.D. Abbott et al., ApJ **848**, L12 (2017)
7. B.P. Abbott, R. Abbott, T.D. Abbott et al., ApJ **848**, L13 (2017)
8. D. Kasen, B. Metzger, J. Barnes, E. Quataert, E. Ramirez-Ruiz, Nature **551**, 80–84 (2017)
9. M. Tanaka, Y. Utsumi, P.A. Mazzali et al., Pub. Astron. Soc. Jpn **69**, 102 (2017)
10. D. Watson, C.J. Hansen, J. Selsing et al., Nature **574**, 497 (2019)
11. J.H. Gillanders, M. McCann, S.A. Sim, S.J. Smartt, C.P. Ballance, MNRAS **506**, 3560 (2021)
12. N. Domoto, M. Tanaka, D. Kato, K. Kawaguchi, K. Hotokezaka, S. Wanajo, ApJ **939**, 8 (2022)
13. S. Goriely, A. Bauswein, H.T. Janka, Astrophys. J. Lett. **738**, L32 (2011)
14. O. Just, A. Bauswein, Pulpillo R. Ardevol, S. Goriely, H.T. Janka, MNRAS **448**, 541 (2015)
15. O. Just, I. Kullmann, S. Goriely, A. Bauswein, H.-T. Janka, C.E. Collins, MNRAS **510**, 2820–2840 (2022)
16. G. Gaigalas, D. Kato, P. Rynkun, L. Radžiūtė, M. Tanaka, ApJS **240**, 29 (2019)
17. G. Gaigalas, P. Rynkun, L. Radžiūtė, D. Kato, M. Tanaka, P. Jönsson, ApJS **248**, 13 (2020)
18. L. Radžiūtė, G. Gaigalas, D. Kato, P. Rynkun, M. Tanaka, ApJS **248**, 17 (2020)
19. H. Carvajal Gallego, P. Palmeri, P. Quinet, MNRAS **501**, 1440 (2021)
20. M. Tanaka, D. Kato, G. Gaigalas, K. Kawaguchi, MNRAS **496**, 1369 (2020)
21. C.J. Fontes, C.L. Fryer, A.L. Hungerford, R.T. Wollaeger, O. Korobkin, MNRAS **493**, 4143 (2020)
22. H. Carvajal Gallego, J.C. Berengut, P. Palmeri, P. Quinet, MNRAS **509**, 6138 (2022)
23. H. Carvajal Gallego, J.C. Berengut, P. Palmeri, P. Quinet, MNRAS **513**, 2302 (2022)
24. H. Carvajal Gallego, J. Deprince, J.C. Berengut, P. Palmeri, P. Quinet, MNRAS **518**, 332–352 (2023)
25. R.F. Silva, J.M. Sampaio, P. Amaro, A. Flörs, G. Martínez-Pinedo, J.P. Marques, Atoms **10**, 18 (2022)
26. A. Flörs, R.F. Silva, J. Deprince, H. Carvajal Gallego, G. Leck, G. Martínez-Pinedo, J.M. Sampaio, P. Amaro, J.P. Marques, S. Goriely, P. Quinet, P. Palmeri, M. Godefroid, Mon. Not. Roy. Astr. Soc., submitted (2023). arXiv:2302.01780 [astro-ph.HE]
27. C.J. Fontes, C.L. Fryer, R.T. Wollaeger, M.R. Mumpower, T.M. Sprouse, MNRAS **519**, 2862 (2023)
28. R.D. Cowan, *The Theory of Atomic Structure and Spectra* (California Univ. Press, Berkeley, 1981)
29. P. Quinet, P. Palmeri, E. Biémont et al., Mon. Not. Roy. Astr. Soc. **307**, 934 (1999)
30. J. Blaise, J.-F. Wyart, Selected Constants Energy Levels and Atomic Spectra of Actinides. Tables internationales de constantes, https://inis.iaea.org/search/search.aspx?orig_q=RN:24031406 (1992)
31. J. Blaise, J.-F. Wyart , http://www.lac.universite-paris-saclay.fr/Data/Database/ (1994)
32. H. Karp, G. Lasher, K.L. Chan, E.E. Salpeter, ApJ **214**, 161 (1977)
33. R.G. Eastman, P.A. Pinto, ApJ **412**, 731 (1993)
34. D. Kasen, R.C. Thomas, P. Nugent, ApJ **651**, 366 (2006)
35. V.V. Sobolev, *Moving Envelopes of Stars* (Harvard Univ. Press, Cambridge, 1960)
36. H. Carvajal Gallego, J. Deprince, M. Godefroid, S. Goriely, P. Palmeri, P. Quinet, European Physical Journal D: Atoms, Molecules, Clusters and Optical Physics. Topical Issue: Atomic and Molecular Data and Their Applications: ICAMDATA 2022, Accepted for publication (2023)
37. E. Biémont, P. Quinet, T.A. Ryabchikova, MNRAS **336**, 1155–1160 (2002)
38. H. Ma, M. Liu, Y. Geng, T. Wang, Z. Yu, H. Zheng, S. Gamrath, P. Quinet, Z. Dai, ApJSS **260**, 56 (2022)
39. S. Fraga, J. Karwowski, K.M.S. Saxena, *Handbook of Atomic Data* (Elsevier, Amsterdam, 1976)
40. Z.S. Li, Z.G. Zhang, V. Lokhnygin, S. Svanberg, T. Bastin, E. Biémont, H.P. Garnir, P. Palmeri, P. Quinet, J. Phys. B: At. Mol. Opt. Phys. **34**, 1349 (2001)

41. E. Biémont, H.P. Garnir, T. Bastin, P. Palmeri, P. Quinet, Z.S. Li, Z.G. Zhang, V. Lokhnygin, S. Svanberg, MNRAS **321**, 481 (2001)
42. Z.G. Zhang, G. Somesfalean, S. Svanberg, P. Palmeri, P. Quinet, E. Biémont, A&A **384**, 364 (2002)
43. S. Gamrath, P. Palmeri, P. Quinet, MNRAS **480**, 4754 (2018)
44. S. Gamrath, M. Godefroid, P. Palmeri, P. Quinet, K. Wang, MNRAS **496**, 4507 (2020)
45. S. Gamrath, P. Palmeri, P. Quinet, Atoms **7**, 38 (2019)
46. K. Kawaguchi, S. Fujibayashi, M. Shibata, M. Tanaka, S. Wanajo, ApJ **913**, 100 (2021)
47. I. Kullmann, S. Goriely, O. Just, A. Bauswein, H.T. Janka, MNRAS, submitted (2023)